

Reshaping of sandstone surfaces by cryptoendolithic cyanobacteria: bioalkalization causes chemical weathering in arid landscapes

B. BÜDEL,¹ B. WEBER,¹ M. KÜHL,² H. PFANZ,³ D. SÜLTEMAYER¹ AND D. WESSELS⁴

¹Botany, Department of Biology, University of Kaiserslautern, PO Box 3049, D-67653 Kaiserslautern, Germany

²Marine Biological Laboratory, Institute of Biology, University of Copenhagen, Strandpromenaden 5, DK-3000 Helsingør, Denmark

³Applied Botany, Department of Bio- and Geo Sciences, University of Duisburg-Essen, Universitätsstraße 5, D-45117 Essen, Germany

⁴Department of Biodiversity, School of Molecular and Life Sciences, University of the North, Private Bag X1106, 0727 Sovenga, South Africa

ABSTRACT

We report a novel weathering mechanism in South African sandstone formations, where cryptoendolithic cyanobacteria induce weathering by substrate alkalization during photosynthesis. As a result, the upper rock part is loosened and then eroded away by physical forces such as wind, water, trampling. This special type of 'exfoliation' is widely distributed and affects the geomorphology of whole sandstone mountain ranges and outcrops across several biomes. We show, that this weathering type is initiated by bioalkalization because of the photosynthesis of cryptoendolithic (i.e. those organisms living in small tight open spaces between the sand grains) cyanobacteria causing pH values high enough to enhance silica solution in the cryptoendolithic zone. As modern cyanobacteria are the initial photoautotrophic colonizers of bare rocks in arid and semiarid landscapes, it is possible that they may also have played a significant role in shaping sandstone landscapes in the geological past.

Received 07 December 2004; accepted 06 January 2005

Corresponding author: B. Büdel, tel.: 49 631 205 2360; fax: 49 631 205 2998; e-mail: buedel@rhrk.uni-kl.de

INTRODUCTION

Weathering of rocks and minerals at the Earth's surface can be divided into three broad categories: chemical, physical and biological. The biologically induced processes result in either physical or chemical reactions. The organisms involved range from bacteria to plants and animals (see review of Barker *et al.*, 1997). Silicate minerals, a major component of natural rocks and residual products of weathering, show an exceptional high resistance against weathering. As bioinduced physical weathering of sandstones is quite well documented (Barker *et al.*, 1997), our knowledge on chemical weathering, induced by living organisms, is rather limited. An earlier report of E.I. Friedmann and coworkers (Friedmann & Weed, 1987; Nienow & Friedmann, 1993) mentions acidification of the habitat by the activity of cryptoendolithic organisms, thus, enhancing weathering rates of the investigated Antarctic sandstone. However, on the basis of natural weathering rates and the recent Earth's temperature regime, Schwartzman & Volk (1989) hypothesized that chemical weathering of silicate

minerals must be considerably enhanced under biotic conditions. Enhancement factors are unknown, but values from 100 to 1000 have been suggested.

In hot and cold deserts, semideserts, savannas, and rain forests of the world, surfaces of silicate rocks, such as sandstone and granite, are regularly colonized by epilithic cyanobacterial biofilms, crusts of cyanolichens as well as cryptoendolithic (for terminology see Golubic *et al.*, 1981) cyanobacteria in natural cavities and pores of the rock (Fig. 1A–F). The cryptoendolithic cyanobacteria always form a distinct blue-green layer 0.5–5 mm below the rock surface (Figs 1C,F; Friedmann *et al.*, 1967; Friedmann, 1980; Friedmann & Ocampo-Friedmann, 1985; Wessels & Büdel, 1995; Weber *et al.*, 1996; Büdel, 1999; Büdel *et al.*, 2000). The layer is restricted to a zone that receives sufficient light to allow positive carbon gain via photosynthesis (Nienow *et al.*, 1988; Vestal, 1988; Weber *et al.*, 1996). Cyanobacteria belonging to the genus *Chroococcidiopsis*, which comprises a few cosmopolitan species, are the most frequent and widespread cryptoendolithic organisms in such systems (Büdel, 1999; Wynn-Williams, 2000; Fewer *et al.*, 2002).

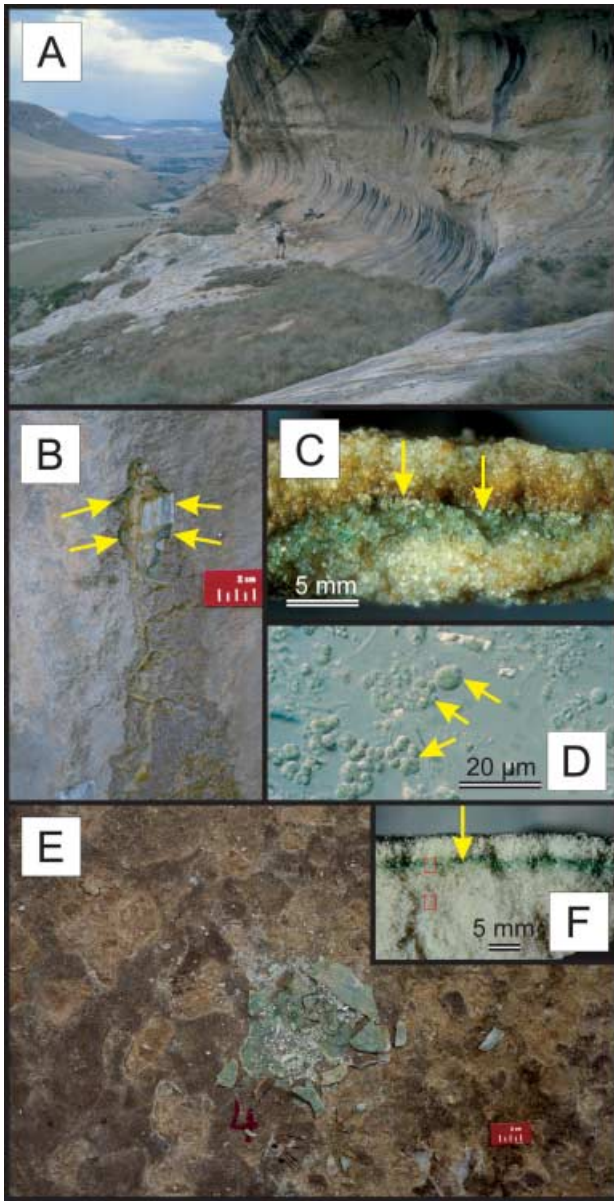


Fig. 1 Clarens sandstone rock formations with cryptoendolithic cyanobacteria. (A–D) Golden Gate Highlands National Park, South Africa. (A) Typical cave ('Holkrans') that gave rise to the former name (Cave sandstone) of the Clarens sandstone formation. The cave surface is completely colonized by endolithic cyanobacteria. (B) Close-up of the cave rock's surface with a part chiselled away. The blue-green band paralleling the surface is visible along the edge (arrows). (C) Cross fracture of the rock, surface on top. A green band of endolithic cyanobacteria can be seen 1–4 mm underneath the surface. Above the cyanobacterial community, a brown zone enriched with ferric oxide is present. Rock splitting is indicated by arrows. (D) Light microscopy of natural population of cyanobacteria from the cryptoendolithic habitat; the unicellular cyanobacterium *Chroococcidiopsis* sp. (arrows) was dominating. (E–F) Tshipise sandstone (subgroup of Clarens formation) at Langjan Nature Reserve, Limpopo Province, South Africa. Rectangles show the region where the samples for the thin sections in Fig. 2 (A and B) were taken. Rock splitting is indicated by an arrow. (E) Close up of the surface of the sandstone outcrop, showing scaled off rock chips and the blue-green colour of the cryptoendolithic cyanobacteria. In the central part of the picture, the upper layer of the rock was removed with hammer and chisel. (F) Cross-fractured rock piece, surface on top. The green band of the cyanobacterial community is located 1–2 mm underneath the surface.

The discovery of extensive cryptoendolithic cyanobacterial growth in sandstones from the Clarens formation in South Africa, associated with it the phenomenon of extensive flaking of the upper rock parts above the endolithic layer, gave rise to the present investigation.

METHODS

Scanning electron microscopy (SEM)

Wet sandstone cubes containing the cryptoendolithic community of about $0.5 \times 0.5 \times 0.5$ cm were fixed for 24 h at 4 °C in 2.5% formaldehyde and then rinsed five times in tap water for 30 min each. After dehydration in acetone steps (30, 50, 70, 90, 100%), samples were critical point dried (CPD 030, BAL-TEC, Balzers Union, Liechtenstein) using CO₂ as medium. The samples were sputter coated with gold (Sputtering Device 07120-A, Balzers Union, Liechtenstein), approximately 30 nm thick. Microscopy was performed using a DSM 962 scanning electron microscope (Zeiss, Germany).

Thin sections

Rock material (Tshipise sandstone) was embedded in epoxide resin (Körapox, Kömmerling Chem. Fabrik KG, Pirmasens, Germany). Samples were then fixed to glass slides and ground down to a thickness of approximately 35 µm. Sections were examined with a light microscope (Axiophot: Zeiss, Oberkochen, Germany) under white and polarized light.

Elemental analysis

Mineral components within rock samples were analysed with an X-ray microprobe system (SX 50, Cameca, Paris) at an acceleration voltage of 15 kV and a ray current of 10 nA performed in a Faraday-cage. The following standards were used: dolomite ([MgCa]CO₃) for Mg, calcite (CaCO₃) for Ca, MnTiO₃ for Mn, ferric oxide (Fe₂O₃) for Fe, and a synthetic andradite (Ca₃Fe₂(SiO₄)₃) for Si. Values were converted into the corresponding compounds using conversion factors according to Küster & Thiel (1985).

Isolation and cultivation of cyanobacteria

Cyanobacteria were isolated from the endolithic environment by scratching them off fractured rock material with sterile forceps in a laminar flow bench. The material was transferred to Petri dishes containing mineral medium (BG11 in 0.9% Agar; Waterbury & Stanier, 1978) and incubated at 16 °C under an irradiance of approximately 60 µmol photons m⁻²s⁻¹ and a light-dark regime of 14 : 10 h. Single cell colonies were repeatedly picked and transferred to fresh medium yielding several uni-cyanobacterial isolates.

Endolithic model system

A Petri dish filled with a 1 cm thick layer of sterile quartz sand (grain size <math><100\ \mu\text{m}</math>) was saturated with liquid mineral medium and inoculated with *Chroococcidiopsis* strains 90.1 and 90.5, respectively. The cultures were incubated at 25 °C under an irradiance of 1000 $\mu\text{mol photons m}^{-2}\text{s}^{-1}$. The initial pH of the medium was 7.5. After 8–10 weeks incubation, the cyanobacteria had disappeared from the surface and formed a visible horizontal green band 1.5–2 mm below the surface (Weber *et al.*, 1996).

Photosynthesis, respiration and pH shift

For measurements of changes in pH and O_2 concentration, cells were collected from liquid cultures by centrifugation (2000 g, 5 min), washed once in assay buffer and finally resuspended in 10 mL of assay buffer containing 1 mM Mes/KOH (pH 8.0), 10 mM NaCl, 1 mM K_2HPO_4 , 4 mM KHCO_3 , and 10 μL carbonic anhydrase (5 mg mL^{-1}). The final Chl *a* concentration in the experimental solution varied between 3 and 5 $\mu\text{g/mL}$. Cells were filled into a thermostated reaction chamber (20 °C, volume = 10 mL), which was attached to a mass spectrometer (Fock & Sültemeyer, 1989) via a semi-permeable membrane inlet system (Wellburn, 1994). The cuvette was closed with a Perspex stopper through which a pH electrode was placed into the cell suspension. Light was provided by a light projector giving a maximal irradiance of approximately 1550 $\mu\text{mol photons m}^{-2}\text{s}^{-1}$. Lower irradiances were realized by inserting calibrated neutral density filters in front of the light source.

Chlorophyll determinations

Chlorophyll was extracted in 1 mL 80% DMSO (dimethylsulfoxide) for 2 h at 65 °C according to the method described in Ronen & Galun (1984). $\text{Mg}_2(\text{OH})_2\text{CO}_3$ was added to avoid acidification and a concomitant pheophytinization of chlorophyll. After spectrophotometry, the chlorophyll content was calculated using the equations of Wellburn (1994).

Microsensor measurements

During microsensor measurements in the endolithic model system, a fibre optic lamp supplied vertically incident collimated light (Schott KL-1500) and the sand was covered by 4–5 mm aerated medium. All microsensors were mounted on a motorized micromanipulator (Märtzhäuser GmbH, Germany) and were inserted in the sand at an opening angle of 135° relative to the incident light. Profile measurements were done in steps of 0.1–0.2 mm vertical depth intervals. The position where the microsensor tips touched the sand surface was determined visually with a dissection microscope.

Positioning of the microsensors and data acquisition of the measuring signals was carried out with a custom made Pascal software on a PC equipped with a motor controller card and an A/D conversion card. Measuring signals were also recorded on a strip-chart recorder. Microprofiles of pH were measured with a pH-glass microelectrode (Revsbech & Jørgensen, 1986) and a standard calomel reference electrode (radiometer); both were connected to a high impedance mV-meter (Keithley 617). Calibration was done at experimental temperature from readings of the microelectrode signal in standard buffers (pH 4.00, 6.88, and 9.22). The pH electrode had a near-Nernstian response of 57.4 mV/(pH unit). Oxygen concentration profiles were measured with a Clark-type oxygen microsensor (Revsbech, 1989) connected to a pA meter. Linear calibration of the microsensor signal was done from pA readings in air-saturated medium (135 pA for 273 $\mu\text{mol O}_2\ \text{L}^{-1}$) and in medium made anoxic by addition of sodium dithionite (<1 pA). The microsensor had a stirring sensitivity of <1% and a t_{90} response time of <0.5 s. Rates of gross photosynthesis were measured at 0.1 mm spatial resolution with the light to dark shift method (Revsbech & Jørgensen, 1986).

RESULTS AND DISCUSSION

Associated with the cryptoendolithic cyanobacterial layer, a loosening of rock flakes with a thickness of about 2 mm (Fig. 1E) can often be observed. This exfoliation process occurs over large areas (in the range of several hectares). We discovered the phenomenon in 1991 in the Clarens sandstone formation of the Drakensberg system (Free State, South Africa, Golden Gate Highlands National Park; Figs 1A–D and 2E) and also studied exfoliation on a large Tshipise sandstone outcrop (Brakrivier, Langjan Nature Reserve, north western Limpopo Province, South Africa; Figs 1E,F). Besides South Africa, we observed exfoliation processes on sandstone rocks in Australia and North and South America; details are listed in Table 1. In all cases, exfoliation was always associated with cryptoendolithic cyanobacteria. The five caves we investigated in the Golden Gate Highlands National Park, and the 9200 m^2 of the sandstone outcrop at Langjan Nature Reserve were entirely colonized by cryptoendolithic cyanobacteria.

The sandstone flakes detach from the rock surface along the blue-green coloured zone (Figs 1C,F). We quantified the exfoliation of Tshipise sandstone over two years (1992 and 1993) in two sites of 624 cm^2 each (Weber *et al.*, 1996). At site 1, 35.7% and 8.6% of the surface area scaled off in 1992 and 1993, respectively, whereas the rates for site 2 were 29.2% and 20.3%. This amounted to 12.7 g and 16.5 g of weathered rock material at the two sites in 1993, respectively. Assuming a mean exfoliation rate of 15 g per year for each investigated area, about 24 kg of rock material could be removed per 100 m^2 per year (=2400 kg per hectare per year) as a result of exfoliation. However, because those are small-scale and

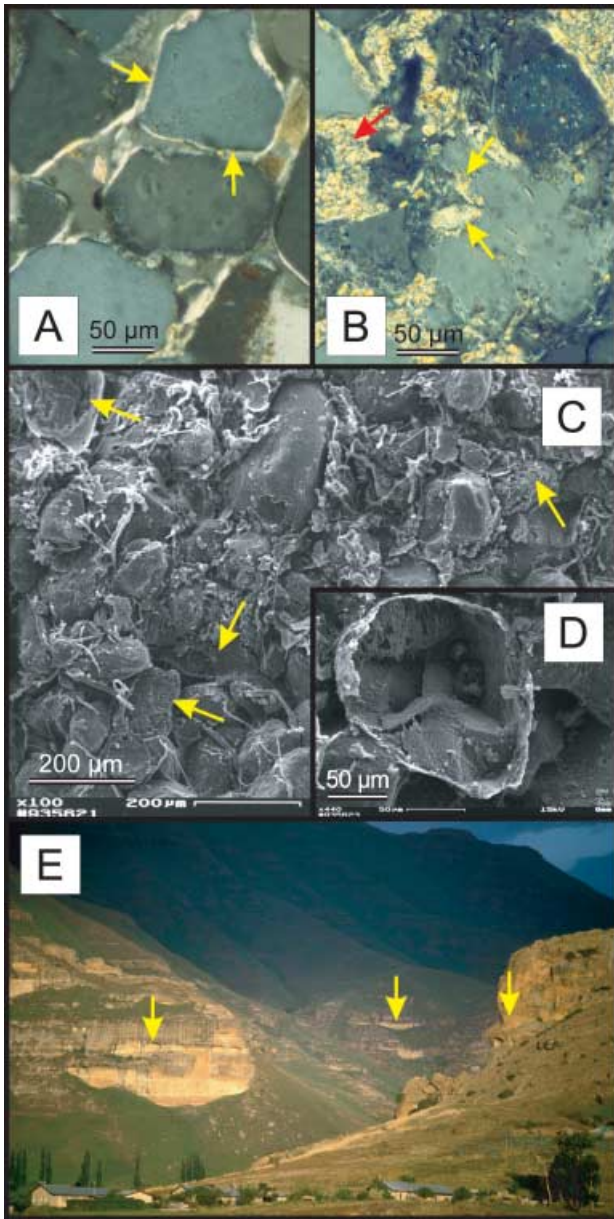


Fig. 2 (A–D) Petrographic thin sections and SEM micrographs of Tshipise sandstone. (A) Noncolonized sandstone from underneath the cyanobacterial community, the quartz grains are round and do not show weathering cavities. Cementing material indicated by arrows. (B) Cross section of the layer colonized by cyanobacteria; yellow arrows indicate erosive cavities, whereas red arrow shows precipitated carbonates (golden colour). (C) SEM micrograph of the colonized blue-green band, showing the quartz grains surrounded by filamentous and unicellular cyanobacteria. The cementing material has mostly disappeared. (D) SEM close up of an eroded quartz grain in the blue-green zone, with remaining EPS/cementing material layer. (E) Large scale effects of bioalkalization in the Golden Gate Highlands National Park at Brandwag, South Africa. Note the numerous caves (arrows) in the rock, formed by the alkalization activity of cryptoendolithic cyanobacteria.

short-term measurements, the extrapolations may represent overestimations.

After exfoliation, the rock flakes are eroded away by crystal growth forces that result in peeling of the rock flakes which are then transported away by localized rain wash (Clarens sandstone at Golden Gate Highlands N.P) or running water (Tshipise sandstone system at Langjan N.R). Exfoliation results in light and dark patches of different shades at the rock surface, caused by sequential weathering (Figs 1A,E). In areas where the brown rock flakes have broken away along the cryptoendolithic zone, the underlying whitish to light-brown rock with the organisms becomes exposed. The cryptoendolithic community subsequently recolonizes such surfaces gradually, leading to the formation of a new brownish surface crust (Fig. 3A). This observed surface pattern is morphologically similar to that described from Beacon sandstone in the Ross Desert, Antarctica (Friedmann & Weed, 1987; Nienow & Friedmann, 1993), although the composition of the cryptoendolithic communities and the weathering mode differ.

Geological thin sections and microprobing

Tshipise sandstone belongs to the Clarens formation that is composed of fine-grained aeolian sandstone, deposited during the late Triassic when aridity reached its maximum (Visser, 1984). In the noncolonized rock below the cyanobacterial zone, the Tshipise sandstone is a well sorted clay-bound sandstone with 0.2–0.4 mm wide oval shaped mineral grains consisting mainly of silicate. Feldspars and micas make up less than 5% of the mineral content. Polarization microscopy on petrographic thin sections (see Methods) enabled us to visualize the clay cementation as a shiny yellow layer surrounding the mineral grains (Fig. 2A).

Organisms within the endolithic zone were not preserved because of the embedding method used for thin sectioning but the endolithic growth zone was clearly visible (Figs 1F and 2B,C). Here the mineral grains were not as smooth as in the noncolonized zone but showed numerous irregularities and dissolution cavities. Some grains were almost completely dissolved by etching (Figs 2B,D). The smooth clayey cementation material was dissolved and substituted by yellow-golden coarse crystals consisting of almost pure CaCO_3 (Fig. 2B), as determined by X-ray elemental analysis (see Methods). A small proportion of the material was composed of dolomite, where Ca^{2+} was substituted by Mg^{2+} ($\text{CaMg}(\text{CO}_3)_2$). The carbonate precipitation however, apparently did not result in re-cementation of the quartz grains.

The etching of quartz grains, the dissolution of cementation material, and the precipitation of CaCO_3 were apparently restricted to the zone harbouring endolithic cyanobacteria, indicating special chemical conditions resulting from the presence or activity of the cyanobacteria. We found that the pH of the natural rock and exfoliated flakes along the cyanobacterial zone of the Clarens sandstone (Golden Gate Highlands N.P)

Table 1 Distribution of cryptoendolithic cyanobacterial growth associated with exfoliative weathering of sandstones (modified from Büdel, 1999)

Locality/habitat	Major rock type	Chlorophyll a content [mg m^{-2}]	Major cyanobacterial taxa
South Africa, Free State, Golden Gate highlands National Park, rock cliffs	Clarens sandstone (subgroup of Clarens formation)	63 ± 19.4 ($n = 4$)	<i>Chroococcidiopsis</i> sp., <i>Gloeotheca</i> sp., <i>Synechococcus</i> sp.
South Africa, Limpopo Province, Langjan Nature Reserve, rock plain	Tshipise sandstone (subgroup of Clarens formation)	29.3 ± 20.4 ($n = 41$)	<i>Chroococcidiopsis</i> sp., <i>Trichocoleus</i> cf. <i>sociatus</i> , <i>Nostochopsis lobatus</i>
Australia, Northern Territory, Uluru (Ayer's Rock), inselberg	Arcose sandstone	48.5 ± 16.3 ($n = 4$)	<i>Chroococcidiopsis</i> sp.
Australia, Northern Territory, Katatjuta (Mt. Olga), inselberg	Arcose sandstone	38.5 ± 20.3 ($n = 4$)	<i>Chroococcidiopsis</i> sp.
Australia, Western Australia, Kalbarri National Park, rock cliffs	quartzitic sandstone	no data	<i>Chroococcidiopsis</i> sp.
North America, U.S.A., Arizona, Colorado Plateau, rock cliffs and plains	Cocconino sandstone	87.3 ± 22.3 ($n = 6$; Bell & Sommerfeld, 1987)	<i>Chroococcidiopsis</i> sp., <i>Gloeotheca</i> sp.
South America, Venezuela, Estado Bolivar, Parque Nacional Canaima, table mountains	Roraima quartzites and sandstones	63 ± 19.7 ($n = 6$)	<i>Chroococcidiopsis</i> sp., <i>Gloeocapsa</i> sp.

was above 9, as measured *in situ* with pH indicator paper. This led us to explore possible correlations between exfoliation and bioalkalization resulting from photosynthesis of endolithic cyanobacteria.

Cyanobacterial community and biomass

The endolithic cyanobacterial community was composed of a number of taxa, including the predominating unicellular *Chroococcidiopsis* sp. (Fig. 1D), the heterocyst containing, filamentous and truly branched *Nostochopsis lobatus*, and the filamentous, nonbranched *Trichocoleus* cf. *sociatus*. Often, the cyanobacterial community was associated by septate, hyaline and brownish coloured fungal hyphae, most probably belonging to the deuteromycete group. Chlorophyll values amounted to $63 \pm 19.4 \text{ mg m}^{-2}$ ($n = 4$) in the Clarens sandstone community (Wessels & Büdel, 1995), and $29.3 \pm 20.4 \text{ mg m}^{-2}$ ($n = 41$) in the Tshipise sandstone community (Weber *et al.*, 1996). These levels are in agreement with previously reported values from endolithic communities (see Table 1; Friedmann *et al.*, 1980; Friedmann, 1980; Bell *et al.*, 1986). Cementing material and extracellular polysaccharides (EPS) from the cyanobacteria often visibly coated quartz grains within the cryptoendolithic zone (Figs 2D and 3B). The endolithic biomass in the Tshipise sandstone community (expressed as carbon content) varied from 4 to 107 g C m^{-2} ($n = 41$), and the nitrogen content ranged from 0.7 and 4.4 g N m^{-2} ($n = 41$). Similar values were reported for sandstones colonized by endoliths in the Mojave and Sonoran Desert (Friedmann, 1980) and in Antarctica (Friedman *et al.*, 1980).

Photosynthesis and pH in liquid pure cultures

We have kept cyanobacterial isolates from the Clarens and Tshipise sandstone in pure cultures since 1991 and found

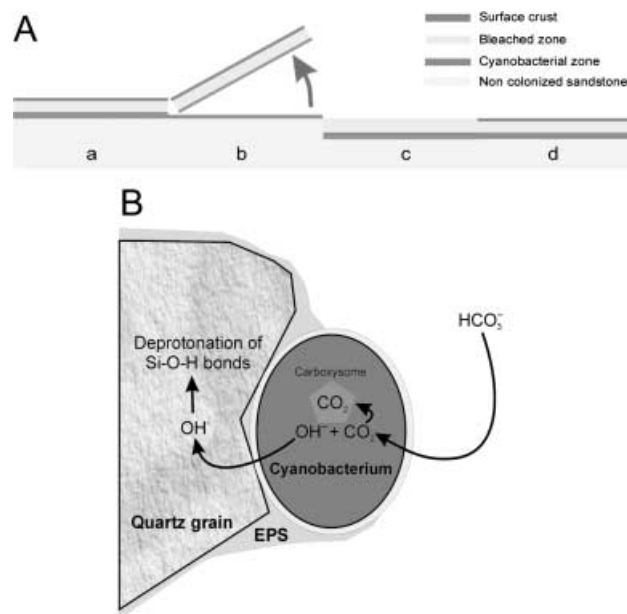


Fig. 3 Schemes of the exfoliation processes. (A) Model of the exfoliation pattern of the Clarens sandstone formation; a = adult cryptoendolithic community with brown surface crust; b = loosening of rock flake and exposure of the cryptoendolithic community; c = withdrawal of the cryptoendolithic community into the rock, start of the bleaching process; d = adult surface crust. (B) Proposed model of the bioalkalization process.

out that the pH in an eight-month-old mass culture of *Chroococcidiopsis* sp. (strain BU 90.1) had increased to almost pH 11. Using two *Chroococcidiopsis* strains (BU 90.1 Clarens sandstone; BU 90.5 Tshipise sandstone), we recorded a pH increase in the liquid medium from pH 6.6 to pH 8.2 within 95 days. Under optimal growth conditions (10 mM HCO_3^-), values of approximately pH 10 were measured in the medium.

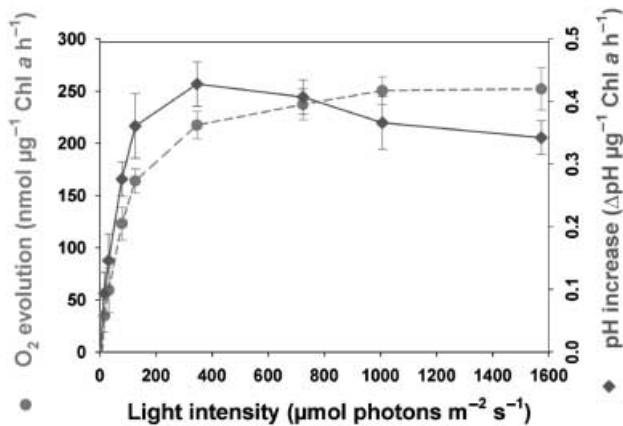


Fig. 4 Rates of photosynthetic O₂ evolution (dots) and pH increase (squares) as a function of irradiance in liquid cultures of *Chroococcidiopsis* strain 90.1 at 25 °C ($n = 5$).

We found a strong correlation between alkalization and photosynthesis in the liquid pure cultures of *Chroococcidiopsis* spp. Simultaneous measurements of net O₂ evolution and pH changes at increasing irradiance (see Methods) showed that pH increased in parallel with photosynthetic oxygen production (Fig. 4). Alkalization of the culture medium was only observed in the light (Fig. 4) and could be stopped by adding the photosynthesis inhibitor 2-(3,4-Dichlorophenyl)-1,1-Dimethylurea (DCMU).

The accumulation of OH⁻ was probably caused by the activation of a CO₂ concentrating mechanism (CCM), in which HCO₃⁻ is actively taken up by several HCO₃⁻ transport options (Price *et al.*, 2002; Shibata *et al.*, 2002). A CCM has been demonstrated in cyanobacteria, where it serves to alleviate CO₂ limitation imposed by low solubility and slow diffusional supply of CO₂ in water (diffusion coefficient 10 000 folds lower than in air; Golubic *et al.*, 1979; Badger & Price, 1992). Internally accumulated HCO₃⁻ serves as a source for CO₂ because it is rapidly dehydrated by a carboxysomal carbonic anhydrase. The resulting OH⁻ is excreted back to the surrounding medium (Fig. 3C; Price *et al.*, 2002; Shibata *et al.*, 2002). The alkalization of pore water within sandstone causes a shift in the carbonate-equilibrium: at pH 8 and above, where CO₂ is largely present as HCO₃⁻ and CO₃²⁻. The carbonate ions can combine with Ca²⁺, but also with Mg²⁺ and Fe²⁺, and precipitate as carbonates within the colonized zone of the sandstone (Fig. 2B, red arrow), but did not cement the quartz grains together again.

Photosynthesis and pH in endolithic model system

The solubility of most rock minerals is pH-dependent (Brunsdén, 1979). Quartz, a framework silicate (SiO₂), is extremely resistant to chemical weathering (Barker *et al.*, 1997), but high pH values, within the range observed in our study, enhance the solubility of silica three to five times. This led us to suspect that

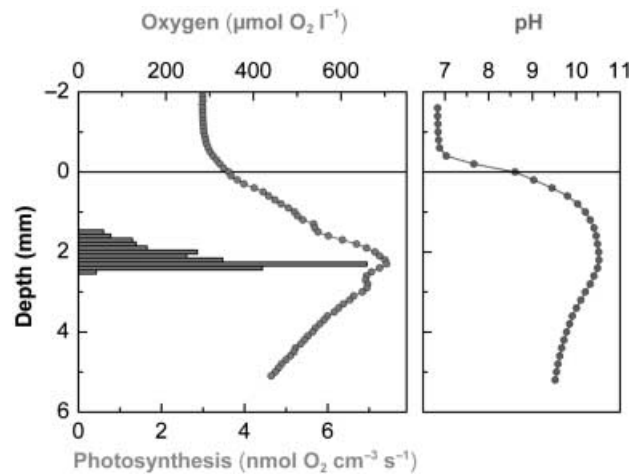


Fig. 5 Microsensor measurements of oxygen (line), photosynthesis (bars) and pH within a quartz sand model system with *Chroococcidiopsis* sp. strain 90.5; 20 °C, irradiance: approximately 500 μmol photons m⁻² s⁻¹.

bioalkalization as a result of photosynthetic activity of endolithic cyanobacteria might be responsible for the observed weathering mechanism (exfoliation). We investigated this possibility further by seeking a tight coupling between alkalization, photosynthetic activity and position within the rock.

Endolithic growth and activity takes place under special microenvironmental conditions (Nienow *et al.*, 1988; Vestal, 1988; Friedmann *et al.*, 1993). Therefore, we investigated the photosynthetic activity and bioalkalization of the endolithic cyanobacteria in a culture model system simulating the endolithic environment. Microsensors were used for measuring oxygen, photosynthesis, and pH distribution in the model system. Mass transport within the water saturated quartz grains of the model system was only by diffusion and in combination with intense endolithic photosynthesis it resulted in a pronounced build-up of oxygen reaching >200% air saturation in the cyanobacterial band 1.5–2.5 mm below the surface. Photosynthesis was confined to this zone with peak activity at 2.2 mm depth (Fig. 5). The photosynthesis caused a significant increase in pH within the model system reaching a maximum of 10.6 within the cyanobacterial zone (Fig. 5). Measurements were performed with two different strains (BU 90.1 and BU 90.5) and yielded similar results. The alkalization was strongly correlated with photosynthesis and followed the oxygen evolution trace, with increased light intensity resulting in higher oxygen evolution and greater pH shift.

The solubility of silicate increases rapidly above pH 9, and our data, thus, clearly show a potential for sandstone weathering (Brunsdén, 1979) as a result of photosynthesis-induced alkalization within the layer of endolithic cyanobacteria. Substrate alkalization has also been reported in a cyanobacterial soil crust community, where a pH shift was correlated with the cyanobacterial photosynthesis and resulted in localized pH values in excess of 10 such as 2–3 units above the soil pH

(Garcia-Pichel & Belnap, 1996). Excretion of OH⁻ during photosynthesis was also observed by Thompson & Ferris (1990).

CONCLUSION

More than 90% of the mineral substance in the Clarens sandstone formation is silica. Acidic dissolution of SiO₂ only occurs at pH values lower than 2 and significantly increases at pH values above 9, [e.g. as a result of deprotonation of Si-O-H bonds (Barker *et al.*, 1997) or hydrolysis reactions (Brunsdon, 1979)]. We found an *in situ* pH of 9.5–10.5 in the Clarens sandstone formation along the endolithic growth zone. The increased weathering of quartz grains, and the removal of the clayey cementation material in this zone can thus be explained by an enhanced mineral solubility within the photosynthetic zone of the endolithic cyanobacteria. Once dissolution of SiO₂ has occurred, leaching processes will remove soluble products, which are transported to the rock surface by evaporation and re-precipitate there to form a brown mineral crust. The rock is weakened in the endolithic growth zone resulting in the formation of rock flakes and subsequent exfoliation. The rock flakes are subsequently eroded away by water flow, crystal forces, or other mechanical impacts. Intermittent swelling of the EPS during water uptake might also play a role for the final loosening of rock flakes.

Biogeochemical weathering of limestone is quite well documented (Degelius, 1962; Danin *et al.*, 1983; Schneider & Le Campion-Alsumard, 1999), whereas the biogeochemical weathering of silicate rocks is less well studied. Friedmann & Weed (1987) described an exfoliative weathering mechanism related to the presence of cryptoendolithic organisms within Beacon sandstone in the Ross Desert of Antarctica. Exfoliation in this system was attributed to a combination of intermittent swelling, freeze expansion, and mobilization of matrix material because of the presence of microorganisms (Friedmann & Weed, 1987; Nienow & Friedmann, 1993), and no bioalkalization was observed. Nevertheless, the weathering patterns at the rock surface in the cold desert of southern Victoria Land, Antarctica reveal a striking morphological (not chemical) similarity to the system we describe here. Confocal laser scanning microscopy studies in combination with the use of a cell-impermeant and pH sensitive dye, revealed a pH < 3.5 in the chasmolithic environment of granites from the Ross Desert, Antarctica (De los Rios *et al.*, 2003). However, because we could show that cyanobacterial alkalization activity is tightly coupled with positive net photosynthesis and disappears during phases of photosynthetic inactivity, pH determination using inactive cyanobacteria (either dead or fixed cells or at light intensities well below compensation) might not be a relevant proof for real pH environments in certain cases.

Bioalkalization is surely not the only mechanism causing exfoliation of silicate rocks, but the bioalkalization process demonstrated here is the first biogeochemical weathering

process directly correlated to the photosynthetic activity of organisms inhabiting silicate rock, a worldwide phenomenon of arid climates and arid microclimatic conditions (Friedmann, 1980; Friedmann & Ocampo-Friedmann, 1985; Büdel, 1999; Wynn-Williams, 2000; see also Table 1). Endolithic cyanobacteria can play a significant role in the weathering of silicate rocks, whereas bioalkalization can have a profound geomorphological influence on a large scale, not only in sandstone formations (Fig. 2E) but possibly also in granite rock outcrops and inselbergs (isolated rises above a plain consist of hard bedrock) harbouring endolithic cyanobacteria under arid climatic or microclimatic conditions around the globe (Büdel, 1999). Furthermore, cyanobacterial soil crusts are widespread in deserts, savannas and steppe formations (Büdel, 2001). Bioalkalization activity (Garcia-Pichel & Belnap, 1996) may also significantly affect soil formation in these biomes.

We found that exfoliation as a result of endolithic cyanobacteria can affect landscape geomorphology. If bioalkalization occurred in ancient communities of terrestrial cyanobacteria, these cryptoendolithic organisms may also have played a significant role in shaping the surface of the Earth on a geological time scale. In fact, biotic enhancement of chemical weathering has been suggested to have played a major role for the habitability of the early Earth (Schwartzman & Volk, 1989).

ACKNOWLEDGEMENTS

The first author would like to thank the DFG (German Research Foundation) for funding. M.K. was funded by the Max-Planck Society and the Danish Natural Science Research Council. D.W. was funded by the University of the North and National Research Foundation. Dr U. Schüssler, University of Würzburg, is thanked for help with the microprobe analysis of the rock minerals. Dr T. G. A. Green, University of Waikato, is thanked for improvement of the English.

REFERENCES

- Badger MR, Price GD (1992) The CO₂ concentrating mechanism in cyanobacteria and microalgae. *Physiologia Plantarum* **84**, 606–615.
- Barker WW, Welch SA, Banfield JF (1997) Biogeochemical weathering of silicate minerals. *Reviews in Mineralogy* **35**, 391–428.
- Bell RA, Athey PV, Sommerfeld MR (1986) Cryptoendolithic algal communities of the Colorado plateau. *Journal of Phycology* **22**, 429–435.
- Bell RA, Sommerfeld MR (1987) Algal biomass and primary production within a temperate zone sandstone. *American Journal of Botany* **74**, 294–297.
- Brunsdon D (1979) Weathering. In *Process in Geomorphology* (eds Embleton C, Thornes J). Edward Arnold Press, London, pp. 73–129.
- Büdel B (1999) Ecology and diversity of rock-inhabiting cyanobacteria in tropical regions. *European Journal of Phycology* **34**, 361–370.
- Büdel B (2001) Synopsis: comparative biogeography and ecology of soil crust biota and communities. In *Biological Soil Crusts* (eds Belnap J, Lange OL). *Ecological Studies*, 150. Springer Berlin, pp. 141–152.

- Büdel B, Becker U, Follmann G, Sterflinger K (2000) Algae, fungi, and lichens on inselbergs. In *Inselbergs* (eds Porembski S, Barthlott W). *Ecological Studies*, 146. Springer Berlin, pp. 69–90.
- Danin A, Gerson R, Garty J (1983) Weathering patterns on hard limestone and dolomite by endolithic lichens and cyanobacteria: supporting evidence for eolian contribution to terra rossa soil. *Soil Science* **136**, 213–217.
- De los Rios A, Wierzychos J, Sancho LG, Ascaso C (2003) Acid microenvironments in microbial biofilms of antarctic endolithic microecosystems. *Environmental Microbiology* **5**, 231–237.
- Degelius G (1962) Über Verwitterung von Kalk- und Dolomitgestein durch Algen und Flechten. Eine Übersicht. In *Chemie Im Dienst der Archäologie, Bautechnik, Denkmalpflege* (ed. Hedvall JA). Hakam Ohlssons, Lund, pp. 156–162.
- Fewer DJ, Friedl T, Büdel B (2002) *Chroococci* and heterocyst-differentiating cyanobacteria are each others closest living relatives. *Molecular Phylogenetics and Evolution* **23**, 82–90.
- Fock H, Sültemeyer DF (1989) O₂ evolution and uptake measurements in plant cells by mass spectrometry. In *Modern Methods of Plant Analysis 9* (eds Liskens HF, Jackson JF). Springer, Berlin, pp. 3–18.
- Friedmann EI (1980) Endolithic microbial life in hot and cold deserts. *Origins of Life* **10**, 223–235.
- Friedmann EI, Kappen L, Meyer MA, Nienow JA (1993) Long-term productivity in the cryptoendolithic microbial community of the Ross Desert, Antarctica. *Microbial Ecology* **25**, 51–69.
- Friedmann EI, LaRock PA, Brunson JO (1980) Adenosine triphosphate (ATP), chlorophyll, and organic nitrogen in endolithic microbial communities and adjacent soils in the dry valleys of southern Victoria land. *Antarctic Journal of the US* **15**, 164–166.
- Friedmann EI, Lipkin Y, Ocampo-Paus R (1967) Desert algae of the Negev (Israel). *Phycologia* **6**, 185–200.
- Friedmann EI, Ocampo-Friedmann R (1985) Blue-green algae in arid cryptoendolithic habitats. *Archiv für Hydrobiologie* Suppl. 71 (*Algological Studies* **38/39**), 349–350.
- Friedmann EI, Weed R (1987) Microbial trace-fossil formation, biogenous, and abiotic weathering in the Antarctic cold desert. *Science* **236**, 703–705.
- Garcia-Pichel F, Belnap J (1996) Microenvironments and microscale productivity of cyanobacterial desert crusts. *Journal of Phycology* **32**, 774–782.
- Golubic S, Friedmann EI, Schneider J (1981) The lithobiontic ecological niche, with special reference to microorganisms. *Journal of Sedimentary Research and Petrology* **51**, 475–478.
- Golubic S, Krumbein W, Schneider J (1979) The carbon cycle. In *Biogeochemical Cycling of Mineral-Forming Elements* (eds Trudinger PA, Swaine DJ). Elsevier Scientific Publishing Company, Amsterdam, Oxford, New York, pp. 29–45.
- Küster FW, Thiel A (1985) *Rechentafeln für die Chemische Analytik*, 103rd edn De Gruyter, Berlin.
- Nienow JA, Friedmann EI (1993) Terrestrial lithophytic (rock) communities. In *Antarctic Microbiology* (ed. Friedmann EI). Wiley-Liss Inc, New York, pp. 343–412.
- Nienow JA, McKay CP, Friedmann EI (1988) The cryptoendolithic microbial environment in the Ross desert of Antarctica: light in the photosynthetically active region. *Microbial Ecology* **16**, 271–289.
- Price GD, Maeda S, Omata T, Badger MR (2002) Modes of active inorganic carbon uptake in the cyanobacterium *Synechococcus* sp. PCC7942. *Functional Plant Biology* **29**, 112–129.
- Revsbech NP (1989) An oxygen microsensor with a guard cathode. *Limnology and Oceanography* **34**, 474–478.
- Revsbech NP, Jørgensen BB (1986) Microelectrodes: their use in microbial ecology. *Adv. Microbial Ecology* **9**, 293–352.
- Ronen R, Galun M (1984) Pigment extraction from lichens with dimethylsulfoxide (DMSO) and estimation of chlorophyll degradation. *Environmental and Experimental Botany* **24**, 239–245.
- Schneider J, Le Campion-Alsumard T (1999) Construction and destruction of carbonates by marine and freshwater cyanobacteria. *European Journal of Phycology* **34**, 417–426.
- Schwartzman DW, Volk T (1989) Biotic enhancement of weathering and the habitability of Earth. *Nature* **340**, 457–460.
- Shibata M, Katoh H, Sonoda M, Ohkawa H, Shimoyama M, Fukuzawa H, Kaplan A, Ogawa T (2002) Genes essential to sodium-dependent bicarbonate transport in cyanobacteria: function and phylogenetic analysis. *Journal of Biological Chemistry* **277**, 18658–18664.
- Thompson JG, Ferris FG (1990) Cyanobacterial precipitation of gypsum, calcite, and magnesite from natural alkaline lake water. *Geology* **18**, 995–998.
- Vestal JR (1988) Carbon metabolism of the cryptoendolithic microbiota from the Antarctic desert. *Applied and Environmental Microbiology* **54**, 960–965.
- Visser DJL (1984) *The Geology of the Republics of South Africa, Transkei, Bophuthatswana, Venda and Ciskei and the Kingdoms of Lesotho and Swaziland*. Geological Survey, Republic of South Africa.
- Waterbury JB, Stanier RY (1978) Patterns of growth and development in pleurocapsalean cyanobacteria. *Microbiological Reviews* **42**, 2–44.
- Weber B, Wessels DCJ, Büdel B (1996) Biology and ecology of cryptoendolithic cyanobacteria of a sandstone outcrop in the northern province in South Africa. *Algological Studies* **83**, 565–579.
- Wellburn AR (1994) The spectral determination of chlorophylls a and b, as well as total carotenoids, using various solvents with spectralphotometers of different resolution. *Journal of Plant Physiology* **144**, 307–313.
- Wessels DCJ, Büdel B (1995) Epilithic and cryptoendolithic cyanobacteria of Clarens sandstone cliffs in the Golden Gate Highlands National Park, South Africa. *Botanica Acta* **108**, 220–226.
- Wynn-Williams DD (2000) Cyanobacteria in deserts – life at the limit?. In *The Ecology of Cyanobacteria – Their Diversity in Time and Space* (eds Whitton BA, Potts M). Kluwer Academic Publishers, Dordrecht, pp. 341–366.